

Electrical and band structural analyses of $\text{Ti}_{1-x}\text{Al}_x\text{O}_y$ films grown by atomic layer deposition on p-type GaAs

This content has been downloaded from IOPscience. Please scroll down to see the full text.

2015 J. Phys. D: Appl. Phys. 48 415302

(<http://iopscience.iop.org/0022-3727/48/41/415302>)

View [the table of contents for this issue](#), or go to the [journal homepage](#) for more

Download details:

IP Address: 115.145.166.68

This content was downloaded on 18/09/2015 at 03:09

Please note that [terms and conditions apply](#).

Electrical and band structural analyses of $\text{Ti}_{1-x}\text{Al}_x\text{O}_y$ films grown by atomic layer deposition on p-type GaAs

Youngseo An¹, Chandreswar Mahata², Changmin Lee¹, Sungho Choi¹,
Young-Chul Byun³, Yu-Seon Kang⁴, Taeyoon Lee², Jiyoung Kim³,
Mann-Ho Cho⁴ and Hyongsu Kim¹

¹ School of Advanced Materials Science and Engineering, Sungkyunkwan University, 2066 Seobu-ro, Jangan-gu, Suwon 440-746, Korea

² Nanobio Device Laboratory, School of Electrical and Electronic Engineering, Yonsei University, 50 Yonsei-ro, Seodaemun-gu, Seoul 120-749, Korea

³ Department of Materials Science and Engineering, The University of Texas at Dallas, 800 West Campbell Road, Richardson, TX 75080, USA

⁴ Institute of Physics and Applied Physics, Yonsei University, 50 Yonsei-ro, Seodaemun-gu, Seoul 120-749, Korea

E-mail: hsubkim@skku.edu

Received 25 March 2015, revised 11 August 2015

Accepted for publication 18 August 2015

Published 17 September 2015



Abstract

Amorphous $\text{Ti}_{1-x}\text{Al}_x\text{O}_y$ films in the Ti-oxide-rich regime ($x < 0.5$) were deposited on p-type GaAs *via* atomic layer deposition with titanium isopropoxide, trimethylaluminum, and H_2O precursor chemistry. The electrical properties and energy band alignments were examined for the resulting materials with their underlying substrates, and significant frequency dispersion was observed in the accumulation region of the Ti-oxide-rich $\text{Ti}_{1-x}\text{Al}_x\text{O}_y$ films. Although a further reduction in the frequency dispersion and leakage current (under gate electron injection) could be somewhat achieved through a greater addition of Al-oxide in the $\text{Ti}_{1-x}\text{Al}_x\text{O}_y$ film, the simultaneous decrease in the dielectric constant proved problematic in finding an optimal composition for application as a gate dielectric on GaAs. The spectroscopic band alignment measurements of the Ti-oxide-rich $\text{Ti}_{1-x}\text{Al}_x\text{O}_y$ films indicated that the band gaps had a rather slow increase with the addition of Al-oxide, which was primarily compensated for by an increase in the valance band offset, while a nearly-constant conduction band offset with a negative electron barrier height was maintained.

Keywords: $\text{Ti}_{1-x}\text{Al}_x\text{O}_y$, atomic layer deposition, GaAs, electrical properties, energy band alignment

(Some figures may appear in colour only in the online journal)

1. Introduction

To further extend the scaling of metal-oxide-semiconductor field-effect transistor (MOSFET) devices, Ge and III-V compound semiconductor technologies have recently been revisited to replace the Si channel due to their higher carrier mobilities [1, 2]. In particular, III-V compound semiconducting channel layers have been considered to be excellent candidates for use in n-channel MOSFETs [2]. However, it is

necessary to integrate high quality high- k gate dielectric films on these III-V compound semiconductors to develop them as a core technology for use in next-generation logic transistors that continue to advance the integrated circuit discipline over the next couple of decades.

There are many possible routes to form ultra-thin high- k gate dielectrics on Si or on higher mobility substrates, and among these, atomic layer deposition (ALD) has been widely adopted for its ability to provide high- k films with superior

Table 1. ALD process conditions for the $\text{Ti}_{1-x}\text{Al}_x\text{O}_y$ films.

Sample number	$(\text{Al}_2\text{O}_3:\text{TiO}_2)_{\text{cycle}} \times$ super cycle	Film stoichiometry (from EDS)
1	(0:264) \times 1	TiO_2
2	(1:10) \times 20	$\text{Ti}_{0.85}\text{Al}_{0.15}\text{O}_y$
3	(1:4) \times 38	$\text{Ti}_{0.69}\text{Al}_{0.31}\text{O}_y$
4	(3:4) \times 20	$\text{Ti}_{0.55}\text{Al}_{0.45}\text{O}_y$
5	(90:0) \times 1	Al_2O_3

interfacial and electrical properties [3]. More importantly, ALD enables facile engineering of the film composition in the depth direction. Since ALD kinetics rely on the nearly-monolayer surface saturation of independently injected precursors [4], a mixed or a nanolaminated film structure can be easily attained using various metal-oxides in order to balance the characteristics of each of the constituting dielectrics. For over a decade, many studies have been carried out on single-layered high- k gate dielectrics (HfO_2 , Al_2O_3 , TiO_2 , etc.), and mixed or nanolaminated films on Si have been extensively synthesized and characterized [5, 6]. Similarly, composition engineering between TiO_2 and Al_2O_3 has also been attempted in mixed [7], bi-layer [8], and tri-layer [9] forms on several III–V substrates to minimize the leakage current while maintaining a high dielectric constant. However, most of these studies have focused only on achieving a specific atomic ratio for Ti and Al in mixed or nanolaminated films without providing sufficient information on the dependence that the final electrical properties and energy band alignment on the III–V substrates have on the composition.

In this study, the compositional effects of $\text{Ti}_{1-x}\text{Al}_x\text{O}_y$ films were investigated by using ALD to prepare films in the Ti-oxide-rich composition range ($x < 0.5$). The MOS capacitors that were built on the p-type GaAs were then characterized in terms of their electrical properties, and furthermore, spectroscopy was used to examine the energy band alignments of the $\text{Ti}_{1-x}\text{Al}_x\text{O}_y$ films with p-type GaAs.

2. Experimental

Prior to ALD, p-type GaAs substrates (Zn-doped at a concentration of $5\text{--}7 \times 10^{17} \text{ cm}^{-3}$) were sequentially cleaned with $\sim 1\%$ hydrofluoric and $\sim 21\%$ $(\text{NH}_4)_2\text{S}$ for 4 and 10 min, respectively. Then, nearly-mixed $\text{Ti}_{1-x}\text{Al}_x\text{O}_y$ films with similar physical thickness were obtained on the pre-cleaned GaAs substrates through nanolamination of atomically-thin TiO_2 and Al_2O_3 layers *via* thermal ALD at 200°C . The ALD rates for the TiO_2 and Al_2O_3 atomic layers were approximately 0.34 \AA/cycle and 1.12 \AA/cycle , respectively, at this temperature. The film composition (i.e. the x value) was carefully controlled by varying the number of cycling ratios of each of the ALD- Al_2O_3 and TiO_2 steps, and nearly identical thicknesses ($9.7\text{--}10 \text{ nm}$) were obtained for all $\text{Ti}_{1-x}\text{Al}_x\text{O}_y$ films by adjusting the total super cycle numbers, as summarized in table 1. Each of the alternating ALD- TiO_2 and Al_2O_3 processes was respectively carried out using titanium isopropoxide (TTIP)/ H_2O and trimethylaluminum (TMA)/ H_2O precursor chemistries. In

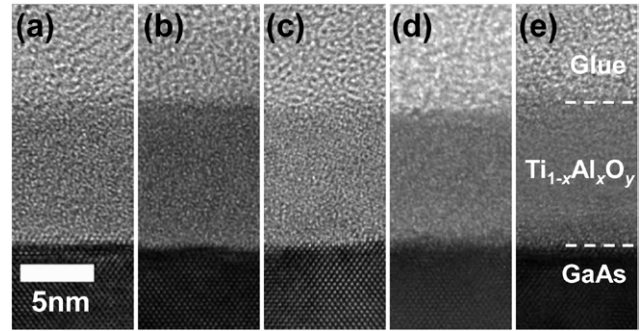


Figure 1. Cross-sectional HRTEM images of the ALD-grown (a) TiO_2 , (b) $\text{Ti}_{0.85}\text{Al}_{0.15}\text{O}_y$, (c) $\text{Ti}_{0.69}\text{Al}_{0.31}\text{O}_y$, (d) $\text{Ti}_{0.55}\text{Al}_{0.45}\text{O}_y$, and (e) Al_2O_3 films on p-type GaAs substrates.

order to improve the interface quality by getting the surface oxides remaining on the wet-cleaned GaAs, all nanolamination processes started with Al_2O_3 formation (TMA injection) [10–12].

Cross-sectional samples were examined under a high-resolution transmission electron microscope (HRTEM, JEOL JEM ARM 200F) to assess the film thickness and microstructure. During the TEM measurements, the approximate film compositions were determined by probing the samples with an energy dispersive x-ray spectroscopy (EDS). Reflection electron energy loss spectroscopy (REELS, VG ESCALAB-210) and x-ray photoelectron spectroscopy (XPS, AXIS-NOVA system located at the Korea Basic Science Institute, Daejeon, Korea) were conducted to analyse the energy band structure of the $\text{Ti}_{1-x}\text{Al}_x\text{O}_y$ films on p-type GaAs.

The dielectric properties of the $\text{Ti}_{1-x}\text{Al}_x\text{O}_y$ films were evaluated by fabricating MOS capacitors to make electrical measurements. Pt top gate electrodes ($\sim 50 \text{ nm}$) were sputter-deposited on the $\text{Ti}_{1-x}\text{Al}_x\text{O}_y$ films and were patterned using a lift-off process, except for the pure Al_2O_3 sample (reference sample) for which a Ni/TaN ($10 \text{ nm}/50 \text{ nm}$) stacked electrode was employed due to adhesion problems of the Pt electrode on Al_2O_3 . Before taking the electrical measurements, all samples underwent post-metallization annealing at 400°C for 30 min in $4\% \text{ H}_2/96\% \text{ N}_2$. The dc sweeping capacitance – voltage ($C - V$) characteristics were measured using an Agilent E4980A LCR meter while the ac frequency that was applied varied from 1 kHz to 1 MHz . The leakage current was also measured using a Keithley 6514 programmable electrometer with a negatively biased gate electrode (electron injection from a gate electrode) with a Keithley 230 programmable voltage source. A series of leakage measurements were taken for each sample with a variation in temperature from 25°C to 125°C by using a temperature-controlled hot-chuck system to gain insight into the conduction mechanism of the leakage current.

3. Result and discussion

Cross-sectional HRTEM images were obtained to determine the thickness and microstructure of the $\text{Ti}_{1-x}\text{Al}_x\text{O}_y$ films (figure 1). The total deposition cycles based on the respective ALD rates of the TiO_2 and Al_2O_3 formation steps were

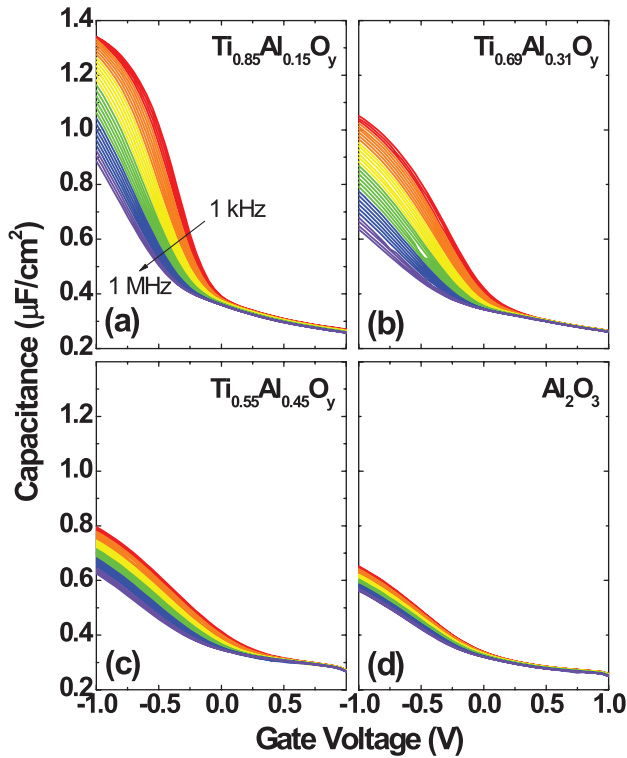


Figure 2. Frequency-dependent C-V characteristics of the ALD-grown (a) $\text{Ti}_{0.85}\text{Al}_{0.15}\text{O}_y$, (b) $\text{Ti}_{0.69}\text{Al}_{0.31}\text{O}_y$, (c) $\text{Ti}_{0.55}\text{Al}_{0.45}\text{O}_y$, and (d) Al_2O_3 films on p-type GaAs substrates measured at room temperature. The ac frequency varied from 1 kHz to 1 MHz.

extensively adjusted to engineer various ALD process recipes for samples with similar thicknesses of about 9.7–10 nm, as verified in the TEM measurements. At an ALD temperature of 200 °C, all the mixed dielectric films, including pure TiO_2 and Al_2O_3 , exhibited an amorphous state regardless of the film composition, which is consistent with other experimental results that have been obtained for Si substrates [13]. The EDS measurements indicate that the compositions of three mixed $\text{Ti}_{1-x}\text{Al}_x\text{O}_y$ films have approximate x values of 0.15, 0.31, and 0.45, implying that most of the mixed samples were within a relatively Ti-oxide-rich composition regime, as intended.

Figure 2 shows the multi-frequency C-V characteristics of the $\text{Ti}_{1-x}\text{Al}_x\text{O}_y$ samples at room temperature, excluding the pure TiO_2 sample due to its high leakage current. The largest frequency dispersion for the accumulation conditions appeared in the sample with the highest amount of Ti-oxide while suppression occurred as the Al-oxide concentration increased. In addition, as a separate experiment, we analysed several nanolaminated TiO_2 - Al_2O_3 films with distinct layer boundaries on GaAs and found that the introduction of a thicker Al_2O_3 layer at the interface suppressed the frequency dispersion [14]. This abnormal frequency dispersion at the accumulation region has usually been observed in ALD-high- k on III-V substrate systems and was attributed to a high density of defects that were located at a few atomic distances close to the substrate, either acting as border traps or generating disorder-induced gap states [15, 16]. Taking this postulation into account, it can be speculated that the Ti-oxide

formation process induces a higher density of near-interface defects than the Al-oxide formation process. Ti is known to have an outstanding oxygen getting property [17], and most recently, Chobpattana *et al* [18] observed significantly suppressed frequency dispersion in accumulation by passivating $\text{In}_{0.53}\text{Ga}_{0.47}\text{As}$ substrates by using an ultra-thin ALD- TiO_2 interfacial layer, which contradicts our results. This may be due to the difference in the Ti precursors that were used for the ALD processes. Different from the tetrakis(dimethylamino) titanium (TDMATi) precursor they used, the TTIP molecule has many oxygen ligands. Therefore, TTIP may have a large tendency to induce unwanted interfacial oxidation (Ga and As-related oxides), which is believed to be the main source of the large frequency dispersion that is observed for highly Ti-oxide-rich samples.

The bi-directional high frequency (10 kHz) C-V curves measured for the MOS capacitors that were fabricated using different $\text{Ti}_{1-x}\text{Al}_x\text{O}_y$ gate dielectrics are compared in figure 3(a). For a more detailed comparison, the apparent dielectric constants (k) were calculated from the measured capacitance values at different frequencies (including the quasi-static measurement) with a gate voltage of -1 V and are plotted as a function of the film composition in figure 3(b). Here, several apparent k values for the highly Ti-oxide-rich samples could not be obtained due to the significant increase in the leakage current. Although it was impossible to extract the exact dielectric constant of the pure TiO_2 film due to its high leakage current, mixing it with Al-oxide results in a decrease in the dielectric constant, as expected. The dielectric constant of the $\text{Ti}_{0.55}\text{Al}_{0.45}\text{O}_y$ film (the least Ti-oxide-rich film in the current sample set) was measured to be of around 12, so the composition range is quite narrow to be able to maintain a higher dielectric constant comparable to that of conventional HfO_2 films, which are widely used as gate dielectrics and have a dielectric constant of ~ 18 [18].

For further electrical characterization, a series of leakage current density versus gate voltage curves were collected at various sample temperatures, and the results are summarized in figure 4. The measurements were taken at a temperature of 25 °C to 125 °C, and the leakage current was traced at a negative gate bias, which corresponds to the gate electron injection condition. At any given measurement temperature, the highest leakage current was observed for the pure TiO_2 sample, while a significant reduction was achieved through the addition of additional Al-oxide, as summarized in figure 4(f). Excluding the pure Al_2O_3 sample, the leakage current of the pure TiO_2 and of all mixed films displayed strong temperature dependence, suggesting that it follows a thermally-activated conduction process with either thermal excitation or thermionic emission of injected electrons. When a certain dielectric film has a small bandgap (i.e. a low barrier height for the electron injection) with a high density of the film defects (i.e. electron traps), its leakage current characteristics are mainly dominated by Schottky emission and Poole-Frenkel conduction, both of which are strongly dependent on the temperature [19, 20]. The temperature and electric field dependencies of the measured leakage current were examined according to theoretical expressions of both conduction mechanisms.

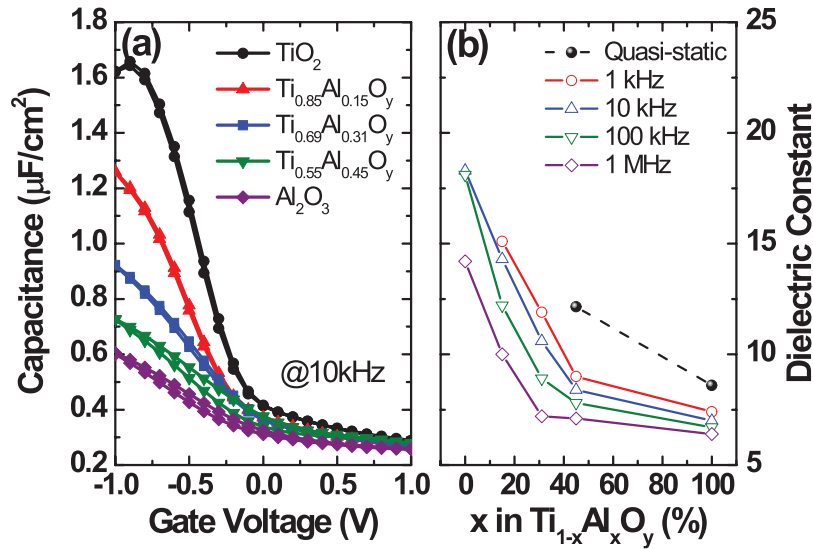


Figure 3. (a) Bi-directional C-V curves of the ALD-grown $Ti_{1-x}Al_xO_y$ films on p-type GaAs substrates measured at a fixed ac frequency of 10 kHz. (b) Variation in the apparent dielectric constant values with the change in the $Ti_{1-x}Al_xO_y$ film composition. The apparent dielectric constant values were estimated from high-frequency and quasi-static capacitances at a gate voltage of -1 V.

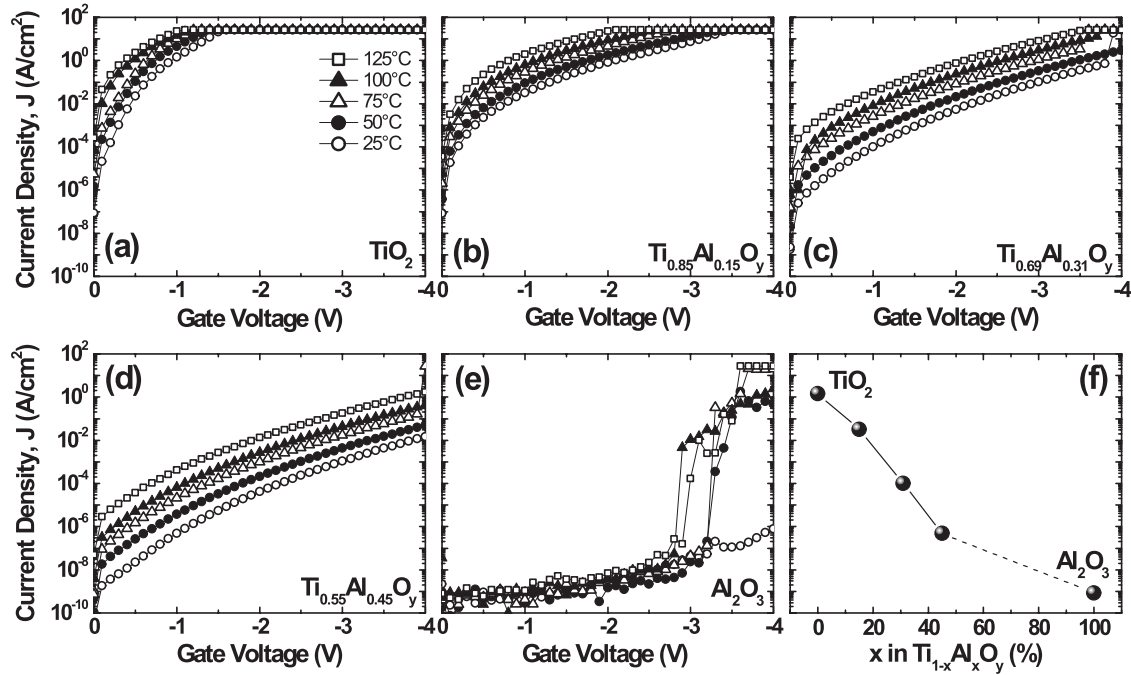


Figure 4. Leakage current characteristics of the ALD-grown (a) TiO_2 , (b) $Ti_{0.85}Al_{0.15}O_y$, (c) $Ti_{0.69}Al_{0.31}O_y$, (d) $Ti_{0.55}Al_{0.45}O_y$, and (e) Al_2O_3 films on p-type GaAs substrates, measured at different temperatures. The measurements were taken under gate electron injection conditions with a variation in temperature from 25 °C to 125 °C. (f) Variation in the leakage current density as a function of the Al-oxide content, measured at 25 °C with a gate bias of -1 V.

However, it was difficult to determine which conduction mechanism was dominant in the mixed $Ti_{1-x}Al_xO_y$ films, as discussed by Jōgi *et al* who experimented using similarly prepared $Ti_{1-x}Al_xO_y$ films on Si substrates [21].

The band alignments of the $Ti_{1-x}Al_xO_y$ films with the p-type GaAs substrates were analysed using REELS and XPS measurements. Figure 5 shows the REELS spectra taken from the films on GaAs, from which the band gap values of the $Ti_{1-x}Al_xO_y$ films were attained by reading the extrapolated edge to a background level. The band gaps estimated for pure

TiO_2 and Al_2O_3 were ~ 3.5 eV and ~ 6.5 eV, respectively, which showed a reasonable agreement with the reported values [22, 23]. The valence band offset (ΔE_V) was calculated using Kraut’s method [24, 25] below to estimate the band discontinuity at the $Ti_{1-x}Al_xO_y$ /GaAs interface with minimal interfacial layer-induced error:

$$\Delta E_V = (E_{CL}^{GaAs} - E_V^{GaAs})_{GaAs} + (E_{CL}^{High-k} - E_{CL}^{GaAs})_{High-k/GaAs} - (E_{CL}^{High-k} - E_V^{High-k})_{High-k} \quad (1)$$

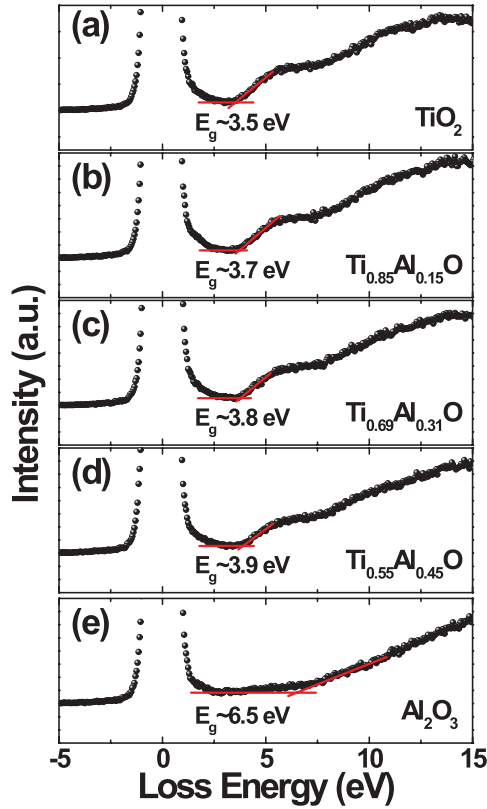


Figure 5. REELS spectra of the ALD-grown $\text{Ti}_{1-x}\text{Al}_x\text{O}_y$ films on p-type GaAs substrates: (a) TiO_2 , (b) $\text{Ti}_{0.85}\text{Al}_{0.15}\text{O}_y$, (c) $\text{Ti}_{0.69}\text{Al}_{0.31}\text{O}_y$, (d) $\text{Ti}_{0.55}\text{Al}_{0.45}\text{O}_y$, and (e) Al_2O_3 films.

Here, E_{CL} and E_{V} represent the core-level energy and the valence band maximum of a specific material (denoted as a superscript), respectively, in a given sample structure (denoted as a subscript of each bracket). Figure 6 shows the valence band and the core level XPS spectra measured from the p-type GaAs substrate and thick $\text{Ti}_{1-x}\text{Al}_x\text{O}_y$ films on GaAs (which are used for all analyses discussed above). The differences between E_{CL} and E_{V} in equation (1) can be determined for both GaAs and $\text{Ti}_{1-x}\text{Al}_x\text{O}_y$, that is, the $(E_{\text{CL}}^{\text{GaAs}} - E_{\text{V}}^{\text{GaAs}})_{\text{GaAs}}$ and $(E_{\text{CL}}^{\text{High-}k} - E_{\text{V}}^{\text{High-}k})_{\text{High-}k}$ values. As the reference core level energy, the As $3d_{5/2}$ peak was used for the GaAs substrate (see figure 6(a)). The Ti $2p_{3/2}$ core level was selected for the mixed $\text{Ti}_{1-x}\text{Al}_x\text{O}_y$ films by including pure TiO_2 (figures 6(b)–(e)), while Al $2p$ was taken for the pure Al_2O_3 film (figure 6(f)). Similarly, the $\Delta E_{\text{CL}}^{\text{High-}k/\text{GaAs}} = (E_{\text{CL}}^{\text{High-}k} - E_{\text{CL}}^{\text{GaAs}})_{\text{High-}k/\text{GaAs}}$ values were obtained by measuring the XPS spectra from additional thin $\text{Ti}_{1-x}\text{Al}_x\text{O}_y$ films (~ 3 nm) prepared on GaAs, which can yield core level spectra coming from both the high- k film and the GaAs substrate, as shown in figure 7. The results in figures 6 and 7 can be combined and entered into equation (1), to calculate the ΔE_{V} values for all $\text{Ti}_{1-x}\text{Al}_x\text{O}_y$ films with different compositions. Furthermore, the conduction band offset (ΔE_{C}) were also calculated using the following equation, which expresses the relationship between ΔE_{V} , the band gap of the GaAs substrate ($E_{\text{g}}(\text{GaAs}) = 1.42$ eV) [20], and the band gap of the $\text{Ti}_{1-x}\text{Al}_x\text{O}_y$ film ($E_{\text{g}}(\text{Ti}_{1-x}\text{Al}_x\text{O}_y)$, as measured from the REELS spectra):

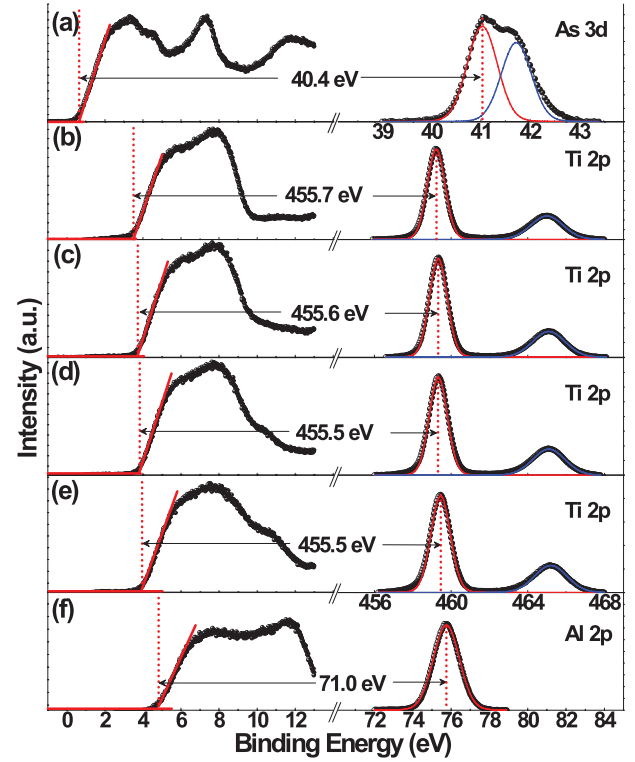


Figure 6. Valence band and core level XPS spectra (symbols) of (a) the p-type GaAs substrate and (b)–(f) thick ALD-grown $\text{Ti}_{1-x}\text{Al}_x\text{O}_y$ films on p-type GaAs substrates: (b) TiO_2 , (c) $\text{Ti}_{0.85}\text{Al}_{0.15}\text{O}_y$, (d) $\text{Ti}_{0.69}\text{Al}_{0.31}\text{O}_y$, (e) $\text{Ti}_{0.55}\text{Al}_{0.45}\text{O}_y$, and (f) Al_2O_3 films. The red lines in the valence band spectra (left) show traces of linear extrapolation to determine the valence band maxima. The red and blue lines in the core level spectra (right) indicate the peak fitting results.

$$\Delta E_{\text{C}} = E_{\text{g}}(\text{Ti}_{1-x}\text{Al}_x\text{O}_y) - \Delta E_{\text{V}} - E_{\text{g}}(\text{GaAs}). \quad (2)$$

The variation in the extracted $E_{\text{g}}(\text{Ti}_{1-x}\text{Al}_x\text{O}_y)$, ΔE_{C} , and ΔE_{V} values of the $\text{Ti}_{1-x}\text{Al}_x\text{O}_y/\text{GaAs}$ heterojunction as a function of the Al-oxide content is shown in figure 8. The band gap of the $\text{Ti}_{1-x}\text{Al}_x\text{O}_y$ films slowly increased within the Ti-oxide-rich regime with x values of less than 0.5 and was mostly dominated by that of Ti-oxide, as observed by Alekhin *et al* [13] for $\text{Ti}_{1-x}\text{Al}_x\text{O}_y$ films on Si substrates. The varying trends in the band offset values as a function of the film composition suggest that the increase in $E_{\text{g}}(\text{Ti}_{1-x}\text{Al}_x\text{O}_y)$ was mainly compensated for by a similarly slow increase in ΔE_{V} with a minimal ΔE_{C} change within the Ti-oxide-rich composition range. In contrast, a much faster increase in the band gap was predicted in the Al-oxide-rich composition regime up to pure Al_2O_3 , which may instead be primarily compensated for by a similar increase in ΔE_{C} . It is notable that the conduction band minimum for GaAs is located at a somewhat higher energy level than that for the Ti-oxide-rich films. Peregó *et al*'s experimentally determined [22] that a similarly negative ΔE_{C} value could be observed in the TiO_2/Si system, and the identity of the interfacial layer between the high- k and Si substrate was revealed to have the ability to tune the ΔE_{C} value. The addition of Al-oxide in the $\text{Ti}_{1-x}\text{Al}_x\text{O}_y$ films (up to $x \sim 0.45$) did not induce a significant increase in ΔE_{C} (instead showing negative values) with respect to p-type GaAs, so it

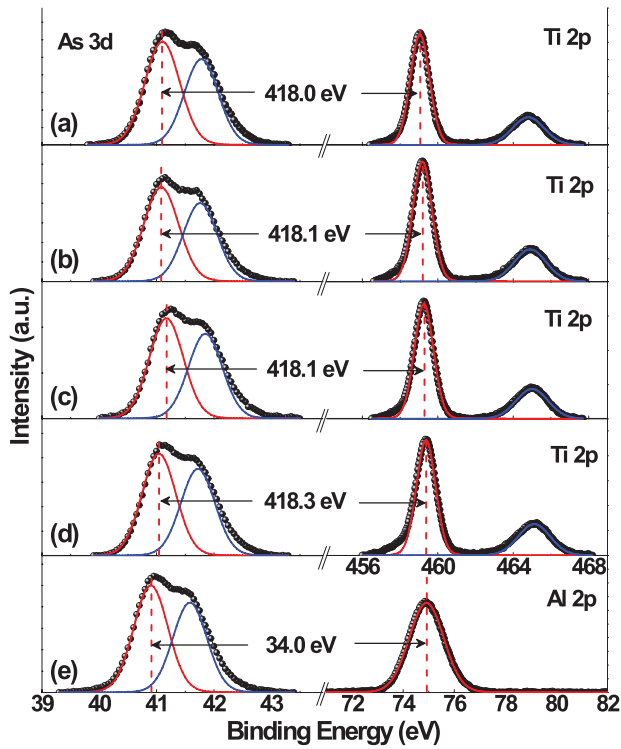


Figure 7. Core level XPS spectra (symbols) measured from thin ALD-grown $Ti_{1-x}Al_xO_y$ films on p-type GaAs substrates: (a) TiO_2 , (b) $Ti_{0.85}Al_{0.15}O_y$, (c) $Ti_{0.69}Al_{0.31}O_y$, (d) $Ti_{0.55}Al_{0.45}O_y$, and (e) Al_2O_3 films. The red and blue lines indicate the peak fitting results.

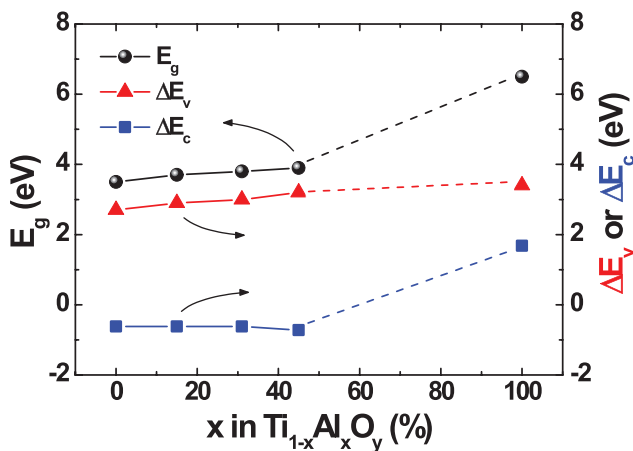


Figure 8. Change in the band gap of the ALD-grown $Ti_{1-x}Al_xO_y$ films (E_g) and in the valance band offset (ΔE_v) and conduction band offset (ΔE_c) with respect to p-type GaAs as a function of the $Ti_{1-x}Al_xO_y$ composition.

may be difficult to reduce the leakage current of the films under substrate electron injection conditions, especially for Schottky emission conduction when an n-type GaAs is used.

4. Conclusion

In summary, we scrutinized the electrical and band structural properties of ALD-grown amorphous $Ti_{1-x}Al_xO_y$ films

on p-type GaAs, particularly within the Ti-oxide-rich composition regime in accordance with x values of less than 0.5. According to the electrical characterization, the ALD- TiO_2 (using TTIP and H_2O chemistry) process-induced high frequency dispersion under accumulation conditions could be relieved by enriching the near-interface region with more Al-oxide, which was accompanied with a simultaneous rapid decrease in the dielectric constant. In terms of the leakage current characteristics, the thermally-activated conduction (Schottky and/or Poole-Frenkel conduction) was dominant in the Ti-oxide-rich regime under gate electron injection conditions while the further addition of Al-oxide helped reduce it. The band alignments for various $Ti_{1-x}Al_xO_y$ films ($x < 0.5$) with p-type GaAs were analysed using REELS and XPS measurements, revealing a slow increase in the $Ti_{1-x}Al_xO_y$ band gap and a valance band offset with the further addition of Al-oxide. Meanwhile, the conduction band offset was somewhat less than zero and was nearly invariant within the range of the Ti-oxide-rich composition.

Acknowledgment

This work was supported by the Future Semiconductor Device Technology Development Program (Grant 10045216) funded by MOTIE (Ministry of Trade, Industry & Energy) and KSRC (Korea Semiconductor Research Consortium). In addition, it was partially supported by the Basic Science Research program (Grant Nos. NRF-2012R1A1A2042548 and NRF-2014R1A4A1008474) through the National Research Foundation of Korea funded by the Ministry of Education and the Ministry of Science, ICT & Future Planning.

References

- [1] Heyns M and Tsai W 2009 *MRS Bull.* **34** 485
- [2] del Alamo J A 2011 *Nature* **479** 317
- [3] Wallace R M, McIntyre P C, Kim J and Nishi Y 2009 *MRS Bull.* **34** 493
- [4] Puurunen R L 2005 *J. Appl. Phys.* **97** 121301
- [5] Wilk G D, Wallace R M and Anthony J M 2001 *J. Appl. Phys.* **89** 5243
- [6] He G, Zhu L, Sun Z, Wan Q and Zhang L 2011 *Prog. Mater. Sci.* **56** 475
- [7] Mahata C et al 2012 *Appl. Phys. Lett.* **100** 062905
- [8] Mukherjee C, Das T, Mahata C, Maiti C K, Chia C K, Chiam S Y, Chi D Z and Dalapati G K 2014 *ACS Appl. Mater. Interfaces* **6** 3263
- [9] Yen C-F, Lee M-K and Lee J-C 2014 *Solid-State Electron.* **92** 1
- [10] Hinkle C L et al 2008 *Appl. Phys. Lett.* **92** 071901
- [11] O'Mahony A et al 2010 *Appl. Phys. Lett.* **97** 052904
- [12] Byun Y-C, An C-H, Lee S-H, Cho M-H and Kim H 2012 *J. Electrochem. Soc.* **159** G6
- [13] Alekhin A P, Choupruk A A, Gudkova S A, Markeev A M, Lebedinskii Yu Yu, Matveyev Yu A and Zenkevich A V 2011 *J. Vac. Sci. Technol. B* **29** 01A302
- [14] An Y and Kim H unpublished results
- [15] Galatage R V, Zhernokletov D M, Dong H, Brennan B, Hinkle C L, Wallace R M and Vogel E M 2014 *J. Appl. Phys.* **116** 014504

- [16] Yuan Y, Yu B, Ahn J, McIntyre P C, Asbeck P M, Rodwell M J W and Taur Y 2012 *IEEE Trans. Electron Devices* **59** 2100
- [17] Kim H, McIntyre P C, Chui C O, Saraswat K C and Stemmer S 2004 *J. Appl. Phys.* **96** 3467
- [18] Chobpattana V, Mikheev E, Zhang J Y, Mates T E and Stemmer S 2014 *J. Appl. Phys.* **116** 124104
- [19] Hori T 1997 *Gate Dielectrics and MOS ULSIs* (New York: Springer) p 45
- [20] Sze S M 1969 *Physics of Semiconductor Devices* (New York: Wiley) p 15, 403
- [21] Jögi I, Kukli K, Kemell M, Ritala M and Leskelä M 2007 *J. Appl. Phys.* **102** 114114
- [22] Perego M, Seguini G, Scarel G, Fanciulli M and Wallrapp F 2008 *J. Appl. Phys.* **103** 043509
- [23] Huang M L, Chang Y C, Chang Y H, Lin T D, Kwo J and Hong M 2009 *Appl. Phys. Lett.* **94** 052106
- [24] Kraut E A, Grant R W, Waldrop J R and Kowalczyk S P 1980 *Phys. Rev. Lett.* **44** 1620
- [25] Kraut E A, Grant R W, Waldrop J R and Kowalczyk S P 1983 *Phys. Rev. B* **28** 1965